Energy 93 (2015) 2503–2517

Contents lists available at ScienceDirect

Energy

journal homepage: www.elsevier.com/locate/energy

Performance assessment of a natural gas expansion plant integrated with a vertical ground-coupled heat pump

Reza Ghezelbash [a, *], Mahmood Farzaneh-Gord [a], Hamidreza Behi [b], Meisam Sadi [c], Heshmatollah Shams Khorramabady [d]

[a] Department of Mechanical Engineering, Shahrood University, Semnan, Iran
[b] Department of Energy Technology, KTH Royal Institute of Technology, SE-100 44 Stockholm, Sweden
[c] Department of Engineering, Islamic Azad University-Shahrood Branch, Semnan, Iran
[d] Lorestan Gas Company, Khorramabad, Iran

ARTICLE INFO

Article history:
Received 16 February 2015
Received in revised form
9 September 2015
Accepted 24 October 2015
Available online xxx

Keywords:
Natural gas expansion plant
Turbo-expander
Ground-coupled heat pump
Energy recovery
Fuel saving

ABSTRACT

In the present paper, a vertical ground-coupled heat pump system is proposed for energy saving in a natural gas expansion plant. Such plant is a modern type of conventional natural gas pressure drop station. Unlike the conventional type, which waste the natural gas pressure exergy in throttling process, the modern one uses the pressure exergy of the natural gas for producing electrical power. A remarkable feature of the proposed system is the type of energy resource used for preheating aim. In previous studies, natural gas was used for the preheating process, however; the proposed system employs geothermal energy as a renewable energy resource for providing part of heating demand. Initially, the vertical ground-coupled heat pump system preheats the natural gas stream up to medium temperatures, then, gas stream passes through station heater and reaches the desired temperature.

For studying the economic and thermal performance of the proposed system, first of all, a system with a high net present value is selected, and then the performance of the selected system is studied in detail. The analysis revealed that the fuel saving potential of the system is 45.80% annually. Economically, the discounted payback period was also calculated about 6 years.

1. Introduction

The majority of global energy is derived from fossil fuels. In recent years, the world trend in reducing dependency on fossil fuels for sustainable development purposes is rapidly rising. Depleting finite fossil fuel resources will be undesirable for the future world (generation). Therefore, it is important to find alternative energy resources. Renewable energies are known as a major alternative to fossil fuels whose emission is much lower than fossil fuel based systems. Geothermal energy is one of the main and most reliable renewable energy resources. It could be divided into high, middle and low-temperature resources. Middle and high-temperature resources are used for direct heating and power generation, respectively. The energy of the both resources comes from the thermal flows produced by the molten core of the earth and is available in a deeper depth of the earth. On the other hand, low-temperature resources could be found just a few meters below the ground which are used for indirect heating. Utilization of the low-temperature geothermal resources is made possible by using open and closed loop ground heat exchangers.

Closed and open loop GHXs (ground heat exchangers) are used for heat rejection or heat extraction from underground. Open loop system uses the groundwater or lake water and closed loop system uses GHXs installed horizontally or vertically in the ground. Vertical GHXs are widely being used for GCHPs (ground coupled heat pumps) in several regions of the world. Compared to Horizontal GHXs it uses less land area [1] and less pumping energy. Moreover, the heat exchange rates per unit length of the vertical GHXs is higher than the straight horizontal heat exchanger pipes [2].

GCHPs offer better performance than other conventional heating and cooling devices which have been proved by experimental studies. Michopoulos et al. [3] studied a three-year operation of the GCHP system. They reported the primary energy required by the GCHP system for heating is lowered by 45% and 97% (period average) compared to that of air-to-water heat pump based and conventional oil boiler respectively. Ozyurt and Ekinci [4]

* Corresponding author.
E-mail address: rghezelbash.68@gmail.com (R. Ghezelbash).

http://dx.doi.org/10.1016/j.energy.2015.10.101
0360-5442/

experimentally investigated the performance of vertical GCHP at one of the coldest climate regions of Turkey. The heat pump COP and system COPs were found to be in the range of 2.43–3.55 and 2.07–3.04, respectively. Zhai and Yang [5] studied the performance of first vertical GCHP installed in archives building in China. GCHP is capable of reducing operating cost by 55.8% and payback period was computed two years. Furthermore, experimental data showed that the average COP of the heat pump in the summer was 4.7, correspondingly, 4.6 in winter and 3.9 in transition seasons.

In addition to the suitability of installing GCHP system in different building types, it has a high potential to be used in industrial sectors. The availability of waste heat in most industries might make the utilization of geothermal heat unfavorable. On the other hand, in some industry sectors, there might not be a considerable waste heat while low-grade heating processes is a demand. Thus, using GCHP could decrease energy consumption in such industries.

Iran's NG (natural gas) delivery system has been extended over 34000 km. Iran is the third largest NG consuming country with the total annual amount of 162.2 billion cubic meters [6]. Transferring this huge amount of NG from the production point to the end consumer is a cost and energy consuming process. To overcome pressure drop in long distances, NG must be transmitted in high pressure pipelines (5–7) MPa, but end-consumers are not able to utilize the high-pressure gas. Therefore NG pressure is reduced to a desirable pressure level in several stages. The major pressure reduction takes place in the pressure drop station that is known as CGS. At this point, the NG pressure reduces up to the pressure level of (1.5–2) MPa, generally 1.7 MPa. In Iran and most of the world, throttling valves are being used for pressure reduction of NG flow in pipelines. In the throttling of high-pressure NG, which is a constant enthalpy process, a large amount of pressure exergy is wasted. Study of Farzaneh-Gord et al. [7] revealed Iran's CGSs can produce 762 MW of electrical power by using turbo-expander. By considering the current status of NG consumption in Iran, which have been increased 1.32 times compared to the conducted study year, electricity generation capacity of CGSs has currently reached to 1 GW. Therefore, it is essential to pay attention to power recovery in CGS.

One of the main problems of using turbo-expander or throttle valve in CGSs is NG temperature drop. By addition of pressure drop at throttling action, the NG temperature also drops. The temperature drop is due to the positive Joule–Thomson coefficient and can be about 4.5–6 °C per MPa of pressure drop. On certain thermodynamic conditions ice-like compounds known as “gas hydrate” forms in pipelines. The undesirable phenomenon of gas hydrate formation is because of water and liquid hydrocarbon presence in NG pipeline transmission. Fouling of the indirect water bath heaters (line heater), internal erosion and corrosion of pipelines and even blocking pipelines are issues related to the formation of hydrate [8]. Typically, there is a minimum allowable temperature for gas passing through CGS. The gas temperature must be always kept higher than the allowable temperature. To prevent this hazardous condition, the NG flow is preheated. In Iran, all of the CGSs use indirect line heaters for this purpose. Commonly, the line heaters have low thermal efficiency [9] and consume a large amount of NG as a fuel source for heating gas flow. Utilizing of turbo-expander instead of throttle valve not only cause to an extreme temperature drop, but also increase heating duty of the line heaters about conventional CGSs.

One MPa pressure drop in turbo-expander leads to (15–20) °C temperature drop, approximately four times higher than the constant enthalpy process (throttle valve). Turbo-expanders are generally used for LNG production or to create very low-temperature gas streams in ethane extraction plants [10]. Because work is extracted from the expanding high-pressure gas, the expansion process closely follows an isentropic process. A wide range of turbo-expander models are available, ranging in size from 75 kW to up to 130 MW [7].

CGS energy issues could be studied from two perspectives: power recovery and reduction of energy consumption in conventional CGS. For the latter case, some limited studies have been reported. Farzaneh-Gord and Kargaran [11] proposed using vortex tube instead of throttling valves in NG pressure reduction stations. Furthermore, Farzaneh-Gord et al. [9] proposed a solar system to provide a part of heat demand in Akand CGS. The study was conducted by assuming an uncontrolled line heater. The economic analysis shown the system net benefit would be coming back after 11 years. A recent study by Farzaneh-Gord et al. [12] revealed that using solar heat with the controllable heater at the Akand CGS gives the annual benefit of 27,011 USD with a capital cost equal to 144,000 USD. The simple and discounted payback period are also determined to be 5.5 and 8 years respectively. Lately, in another work, Farzaneh-Gord et al. [13] proposed and studied using of vertical ground heat exchangers in CGSs to reduce fuel consumption in Gonbad Kavoos CGS. Comprehensive thermo-economic analysis showed that a system comprising 8 boreholes with 150 m depth and 0.15 m diameter each is the most efficient configuration for Gonbad Kavoos station. the discounted payback period and IRR of the system was computed to be about 5 years and 15.5% respectively. In comparison with utilizing solar systems, the offered system showed good economic performance.

Most studies have been proposed using turbo-expander for recovering energy of high-pressure NG [14]. In this case, preheating or post-heating of gas flow is accomplished by an industrial waste heat, gas boiler, fuel cell waste heat, ICE (internal combustion engine) waste heat and integration with a refrigeration system.

Farzaneh-Gord and Maghrebi [15] studied exergy destruction in Iran's NG fields. They concluded that one could generate 4200 MW of electricity from this pressure exergy. Farzaneh-Gord and Deymi [16] investigated a performance of Khangiran refinery gas turbines by employing turbo-expander in the pressure drop station of the refinery. They proposed low-temperature gas stream of turbo-expander used to cool inlet air of the gas turbine. The proposed system showed the performance could be improved in the range of 1.5–5% for almost 10 months. Sanaye and Nasab [17] offered using ICE with turbo-expander. The authors optimized the actual annual benefit with nine decision variables and obtained an optimum required number of equipment. Other authors also evaluated the integration of ICE with turbo-expander. Howard et al. [18] offered a system based on molten carbonate fuel cell and turbo-expander. The fuel cell consumes NG and produces high-quality heat in addition to electricity to preheat the NG stream prior to turbo-expander. Kostowski and Usón [19] proposed and evaluated an innovative Power recovery system for NG expansion, based on the integration of ICE and an ORC (Organic Rankin Cycle). NG preheating prior to expansion was carried out partially directly by the ICE cooling cycle, and partially indirectly, using the engine exhaust gases which supply heat for the ORC. Farzaneh-Gord and Jannatabadi [20] conducted an advanced numerical simulation for thermodynamic modeling of NG single acting reciprocating expansion engine. They studied the effect of some parameters on the system: the inlet port diameter, connecting rod length, crank radius, and engine speed. Alparsalan Neseli et al. [21] studied electricity generation potential of the Izmir CGS in energy and exergy point of view. Maximum estimated electricity generation by the system was computed 6365336 kWh. Maximum energy and exergy efficiency were also determined 94.96% and 70.61% respectively. Arabkoohsar et al. [22] employed solar hating system with turbo-expander in

order to reduce fuel consumption in Birjand CGS. NPV (net present value) analysis showed the discounted payback period for the system is equal to 3.5 years.

The previous studies were proposed different systems for power production in the conventional CGSs, which use NG for preheating the expander upstream. The heating value of NG is high and added value of materials derived from this energy source could increase the export earnings of each country. Thus, wasting this reliable energy source in the NGEP (nural gas expansion plant) is undesirable. In this study, an innovative system for preheating turbo-expander upstream is proposed. The proposed system uses vertical GCHP as a sustainable solution for providing part of the preheating energy in NGEP.

2. System descriptions

This section presents a detailed description of the proposed system. As it was claimed, the proposed system takes the advantage of vertical GCHP to provide a portion of the required heat in the NGEP. GHX systems are generally included one or multiple vertical boreholes. The typical boreholes have a diameter about 10–15 cm and 100–200 m long [23]. Heat pumps are connected to the ground via u-tube inserted into the boreholes. The fluid circulates through closed loop and rejects heat to the ground (cooling mode) or absorbs heat from it (heating mode).

Fig. 1 shows the schematic of conventional CGS, NGEP and proposed system integrated to the CGS. The proposed system consists of turbo-expander, line heater, shell and tube heat exchanger and vertical GCHP. The NG must be complete the preheating process through the proposed system Fig. 1C. In contrast with the conventional configuration, wherein the preheating is a one-step process, in the heat pump coupled NGEP (HPC-NGEP) the preheating is performed in two stages.

First, the NG stream enters the shell and tube heat exchanger and warmed up with vertical GCHP. The first heating process is placed to increase the NG temperature by using the proposed heat pump. Seconds, it enters into the line heater where heated up to the desired temperature (th temperature at which risk of freezing is very low). The upstream temperature of the turbo-expander is a function of its downstream temperature, upstream pressure, the composition of NG and isentropic efficiency. The turbo-expander downstream temperature must always be higher than the minimum allowable temperature, i.e. hydrate formation temperature, as mentioned in the introduction section. Hence, it is essential to determine hydrate formation temperature based on NG composition and the pressure level at the outlet of CGS.

Heat pumps need for an external power source to transfer ground heat to the shell and tube heat exchanger. In the proposed system, turbo-expander provides the required electricity of GCHP besides the electricity of pumps used for fluid circulation. Iran has only one commercial company which sipplies GCHPs in country. Maximum water temperature provided by this heat pump is 55 °C, based on the inlet fluid temperature of 49 °C to the condenser. Therefore, the water in temperature of 55 °C supplied by GCHP is pumped to the shell and tube heat exchanger to warm the NG up. When the water cools down, and the temperature decreases to 49 °C, water returns to the heat pump condenser. The minimum and maximum source side fluid temperature has been determined by the manufacturer, −7 °C and 44 °C. Given that the heat pump will always operate in heating mode the possibility of falling fluid

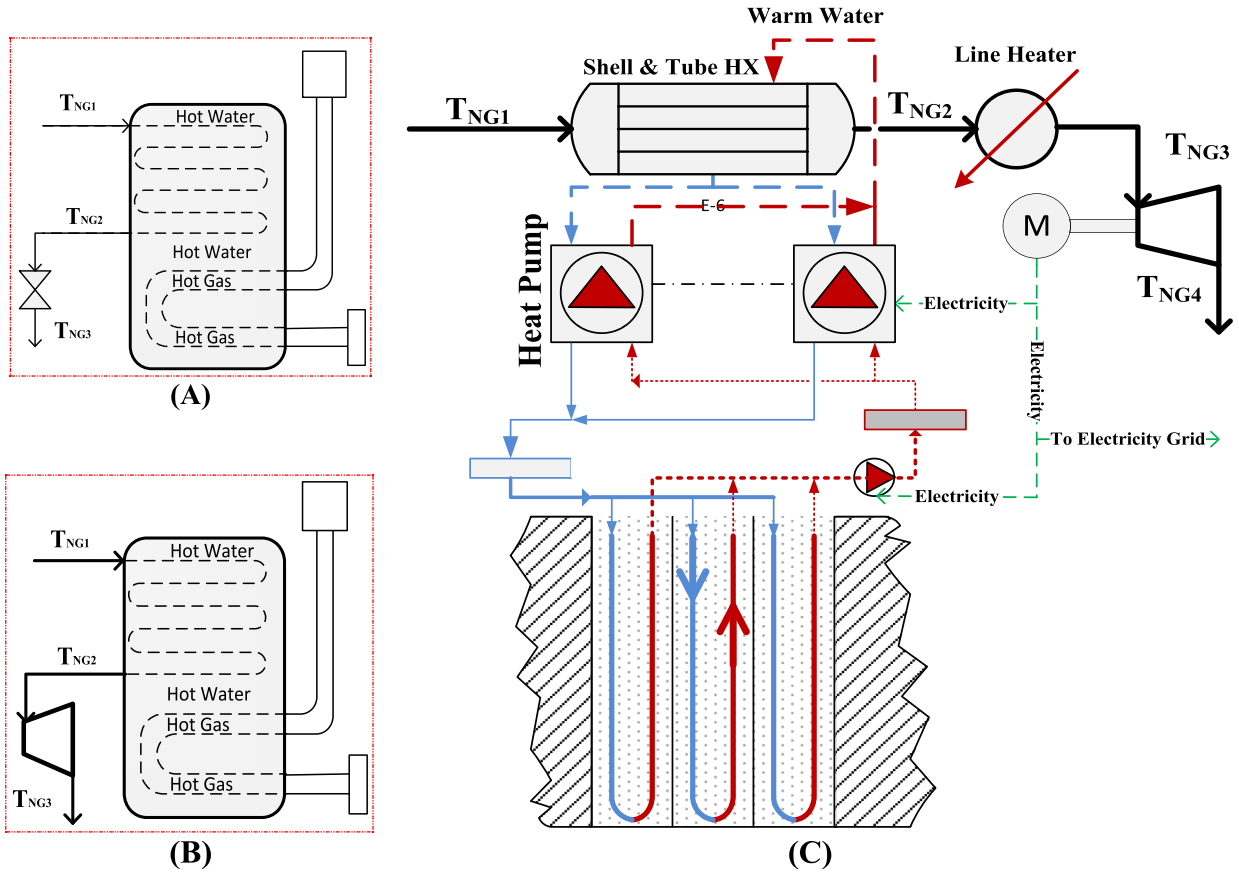

Fig. 1. A) Schematic of CGS, B) Schematic of conventional NGEP and C) Schematic of improved configuration of NGEP; heat pump coupled NGEP (HPC-NGEP).

temperature below than 0 °C is high. Consequently, antifreeze solution must be used as a heat carrier fluid in the source side of the heat pump, i.e. ground loop, to protect against freezing of water.

3. Mathematical modeling

3.1. Turbo-expander and line heater

For computing required energy of line heater and the power produced by expander the inlet NG temperature into the turbo-expander must be determined [17]:

$$T_{NG3} = \frac{T_{NG4}}{1 - \eta_{ex} \cdot \left(1 - \left(\frac{P_{NG4}}{P_{NG3}}\right)^{\frac{\gamma-1}{\gamma}}\right)} \tag{1}$$

T_{NG3} and P_{NG3} are the turbo-expander upstream temperature and pressure. T_{NG4} and P_{NG4} are also the turbo-expander downstream temperature and pressure respectively. η_{ex} is the isentropic efficiency of turbo-expander. Turbo-expander efficiency has also typical value of 84%–86%, which the efficiency of 85% selected for this study. Power output of turbo-expander:

$$W_{ex} = \dot{m}_{NG} \cdot (h_{NG3} - h_{NG4}) \tag{2}$$

By considering efficiency for gearbox (η_{gear}) and generator (η_{gen}), electrical power output from the turbo-expander system could be written as follows:

$$P_{elec} = W_{ex} \cdot \eta_{gear} \cdot \eta_{gen} \tag{3}$$

h_{NG3} and h_{NG4} are the turbo-expander upstream and downstream enthalpy respectively. $\dot{m}_{NG}$ is the NG mass flow rate. The NG thermodynamic properties are calculated with correlations developed by Farzaneh-Gord and Rahbari [24].

The developed correlations for enthalpy, density and Z factor are presented in the common form of Eq. (4). All the properties could be calculated using Eq. (4) except entropy and Joule–Thomson coefficient which are computed by Eq. (8).

$$\begin{aligned} \text{Properties}\ (T', P', \gamma') = {} & A_1(T', \gamma')P'^4 + A_2(T', \gamma')P'^3 + A_3(T', \gamma')P'^2 \\ & + A_4(T', \gamma')P' + A_5(T', \gamma')P'^4 \end{aligned} \tag{4}$$

where $A_i(T', \gamma')$; $i = 1,\ldots,5$ are defined as:

$$A(T', \gamma') = B_1(T')\gamma'^2 + B_2(T')\gamma' + B_3(T') \tag{5}$$

and $B_j(T')$; j = 1,2,3 for each $A_i(T', \gamma')$ are defined as:

$$B(T') = C_1 T'^2 + C_2 T' + C_3 \tag{6}$$

T', P', γ' are functions of temperature, pressure and gas specific gravity respectively and defined as:

$$T' = \frac{T - 300}{50}, \quad P' = \frac{P - 13}{7.3598}, \quad \gamma' = \frac{\gamma - 0.62541}{0.07894} \tag{7}$$

$$0.2 < P(MPa) < 25, \quad 250 < T(K) < 350, \quad \gamma = \frac{Mw}{28.966} \tag{8}$$

γ is the NG specific gravity, Mw is molecular weight of NG and 28.966 is molecular weight of air. The entropy and Joule–Thomson coefficient are correlated as:

$$\begin{aligned} \text{Properties}\ (T', P', \gamma') = {} & A_1(T', \gamma')P'^6 + A_2(T', \gamma')P'^5 \\ & + A_3(T', \gamma')P'^4 + A_4(T', \gamma')P'^3 \\ & + A_5(T', \gamma')P'^2 + A_6(T', \gamma')P' + A_7(T', \gamma') \end{aligned} \tag{9}$$

In which, $A_i(T', \gamma')$; $i = 1,\ldots,7$ are defined by Eq. (5). The coefficients of correlations were listed by Farzaneh-Gord and Rahbari [24].

The rate of required energy of the NG stream for being warmed up could be calculated as below:

$$\dot{Q}_{NG} = \dot{m}_{NG} \cdot (h_{NG2} - h_{NG3}) \tag{10}$$

The heating duty of the heater is provided by burning NG as fuel. Considering the thermal efficiency of the heater, η_h, the fuel mass flow rate, $\dot{m}_{fuel}$, could be calculated as below:

$$\dot{m}_{fuel} = \frac{\dot{Q}_{NG} + \frac{m_w C_w (T_w^{i+1} - T_w^i)}{3600}}{\eta_h \cdot LHV} \tag{11}$$

In which, LHV, m_w and C_w are the lowering heating value of the fuel, the heater water mass and thermal capacity respectively. The thermal efficiency of the line heater is in the range of 35%–50% [9]. In this work, the thermal efficiency of the heater was assumed to be 40%. Also the subscripts (i) and ($i + 1$) stand for the period number.

T_w also refers to the heater water temperature. The immersed coil in water bath could be considered as a pipe in a constant temperature environment, Fig. 2. Thus, based on the correlation presented by Incropera and Dewitt [25], T_w could be calculated from Eq. (16). The energy blance on a differential control volume shown in a Fig. 2B gives:

$$\dot{m} C_p dT_m = h(T_s - T_m) dA_s \tag{12}$$

T_m is the mean temperature of the fluid. dA_s is the differential surface area and equal to pdx, where p is the perimeter of the tube. The relation bove can be rearranged as:

$$\frac{d(T_s - T_m)}{(T_s - T_m)} = -\frac{hp}{\dot{m} C_p} dx, \quad T_s = constant \tag{13}$$

Integrating from $x = 0$ to $x = L$ gives:

$$ln \frac{(T_s - T_e)}{(T_s - T_i)} = -\frac{hA_s}{\dot{m} C_p} \tag{14}$$

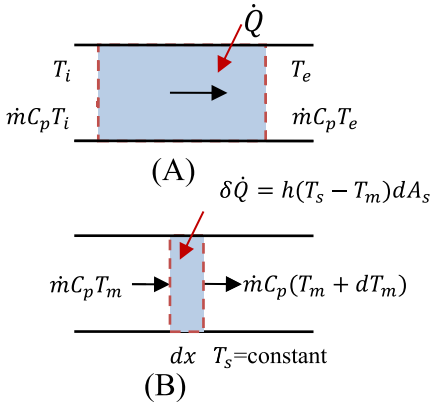

Fig. 2. A) Heat transfer to a fluid flowing in a tube, B) Energy interactions for a differential control volume in a tube.

By substituating T_w, T_{NG1}, T_{NG2}, $\dot{m}_{NG}$, $C_{p,NG}$ instead of T_s, T_i, T_e, $\dot{m}$, C_p the relation above changes to:

$$\frac{T_w - T_{NG2}}{T_w - T_{NG1}} = \exp(Y), \quad Y = \frac{-\pi D_{oc} L_c U_c}{\dot{m}_{NG} \cdot C_{p,NG}} \tag{15}$$

where, D_{oc}, U_c and L_c are the external diameter, length and overall heat transfer coefficient of the coil respectively. Rearranging the above equation to define T_w, one could derieve the following equation:

$$T_w = \frac{T_{NG3} - T_{NG2} \cdot \exp(Y)}{1 - exp(Y)} \tag{16}$$

The previous studies showed that the line heaters with $U_c = 568\ W/m^2\ K$ are acceptable [9]. Employing the formulation presented above, the detailed energy analysis on the NGEP would be possible.

3.2. Vertical GCHP

In this study, heat transfer for inside and outside of the boreholes are modeled separately, with the borehole wall acting as the interface. The model for the borehole interior uses steady state heat transfer [26], but the outside model must take care of the thermal phenomenon from the borehole wall to the surrounding soil and the other boreholes. One could use analytical and numerical models to study heat transfer outside the borehole. Compared to numerical models, analytical models [27] have a low computational time and are flexible in programming. Therefore, it could be the best choice for feasibility studies such as present study. Analytical models are based on ILS (infinite line heat source) [28], CS (cylindrical heat source) [26] and FLS (finite line source) [29].

The ILS and CS were generally used to model heat transfer around the boreholes. The both methods offer a 1D solution to heat transfer from a heat source. The models neglect the axial heat transfer. This assumption cause to overestimation of borehole wall temperature for times greater than 3 years [30]. On the other hand, FLS solution can predict 2D heat transfer from a finite length source positioned in a semi-infinite medium and subjected to a constant heat transfer rate. Eskilson [31] proposed the analytical solution of the FLS. Zeng et al. [29] presented a new methodology to evaluate the temperature in a bore field using the FLS. Contrary to Eskilson work in which the temperature was calculated at mid-height of the source, they used the integral mean temperature over the borehole height and it showed better results. Lamarche and Beauchamp [32] simplified the double integral into a single integral in the FLS solution which led to reducing the time required to calculate the integral mean temperature over the borehole height considerably. Claesson and Javed [33] obtained a correlation to predict the integral average temperature of geothermal bore field where boreholes are buried at a distance D from the ground surface. In contrast to Zeng et al. [29] and Lamarche and Beauchamp [32], the FLS was defined by point heat source integral which was initially integrated into space. Then after, the obtained solution is given in the form of an integral in the time domain.

The FLS by Claesson and Javed [33] is used in this study. Because it provided us with a simpler formulation of the FLS method and compared to ILS and CS, it gives an accurate solution in long time.

3.2.1. Borehole wall temperature at a constant heat flux

Claesson and Javed [33] offered the below formulation for the integral mean temperature at a distance r of a FLS extending from $Z = D$ to $Z = D + H$. The heat source has a strength q_0. The average borehole wall temperature, T_{bw} for the entire set of N boreholes is:

$$T_{bw}(t) - T_g = \Delta T(t) = \frac{q_0}{4\pi k} \cdot \int_{\frac{1}{\sqrt{4\alpha t}}}^{\infty} I_e(s) \cdot \frac{I_{ls}(Hs, Ds)}{Hs^2} \cdot ds \tag{17}$$

In which the T_g in the undisturbed ground temperature, q_0 is the constant ground heat load, k is the ground thermal conductivity, α, H and D are ground thermal diffusivity, borehole active length and borehole inactive length respectively.

$$I_e(s) = \frac{1}{N} \sum_{i=1}^{N} \sum_{j=1}^{N} \exp\left(- r_{i,j}^2 s^2 \right) \tag{18}$$

$r_{i,j}$ denotes the radial distance between borehole i and j ($i \neq j$). The contribution of any heat source related to borehole i is obtained for the radial distance r_b.

$$r_{i,j} = \sqrt{(x_i - x_j)^2 + \left(y_i - y_j\right)^2} \qquad i \neq j \tag{19}$$

$$I_{ls}(h, d) = 2 \cdot ierf(h) + 2 \cdot ierf(h + 2d) - ierf(2h + 2d) - ierf(2d) \tag{20}$$

3.2.2. Borehole wall temperature at a variable heat flux

For a time varying heat flux, $q(t)$, borehole wall temperature is predicted by temporal superposition principle [34].

$$\Delta T(t) = \sum_{j=1}^{n_t} \frac{q_j - q_{j-1}}{4\pi k} \cdot \int_{\frac{1}{\sqrt{4\alpha\left(t - t_{j-1}\right)}}}^{\infty} I_e \cdot \frac{I_{ls}(Hs,\ Ds)}{Hs^2} \cdot ds \tag{21}$$

j is the time step index and n_t is the number of time steps before time t. Eq. (21) could be rewritten as convolution product [35]

$$\Delta T(t) = \sum_{j=1}^{n_t} h(t_j) \cdot f(t - t_{j-1}) = (h * f)(t) \tag{22}$$

Where the $h(t_j)$ is the incremental heat flux function:

$$h(t_j) = q(t_j) - q(t_{j-1}) \tag{23}$$

$$f(t - t_{j-1}) = \frac{1}{4\pi k} \cdot \int_{\frac{1}{\sqrt{4\alpha\left(t - t_{j-1}\right)}}}^{\infty} I_e \cdot \frac{I_{ls}(Hs,\ Ds)}{Hs^2} \cdot ds \tag{24}$$

Marcotte and Pasquier [35] showed that Eq. (22) could be computed with a spectral method using discrete Fourier approach:

$$\Delta T(t) = \mathrm{F}^{-1}(\mathrm{F}(h) \cdot \mathrm{F}(f)) \tag{25}$$

3.2.3. Computing the fluid temperature into the vertical GHXs

Once T_{bw} was calculated at the constant ground thermal load, the temperatures of circulating fluid can be obtained by the concept of thermal resistance, R_b is the borehole thermal resistance.

$$T_f(t) = T_{bw}(t) + q \cdot R_b \tag{26}$$

$$T_{f,in}(t) = T_f(t) - \frac{q \cdot H}{2\dot{m}_f c_f} \tag{27}$$

$$T_{f,out}(t) = T_f(t) + \frac{q \cdot H}{2\dot{m}_f c_f} \tag{28}$$

3.2.4. Borehole interior thermal resistance

Since the thermal capacitance of the borehole compared to adjacent ground is relatively small, heat transfer from borehole wall to the fluid is considered steady state [26]. Thermal resistance inside the borehole includes the thermal resistance of fluid convection, and that of solid conduction in the pipe and grout. Conduction thermal resistance of pipe and the convection thermal resistance of fluid into the pipe are obtained by Eqs. (30) and (31) respectively:

$$R_b = \frac{1}{2}(R_{conv} + R_{cond}) + R_{grout} \tag{29}$$

$$R_{cond} = \frac{\ln\left(\frac{d_o}{d_i}\right)}{2\pi k_{pipe}} \tag{30}$$

$$R_{conv} = \frac{1}{\pi d_{in} h} \tag{31}$$

h is a function of the Nusselt number (Nu). Nu is determined according to the flow regime. By increasing the turbulence of the flow, the convective thermal resistance drops and consequently heat transfer between soil and VGHX enhances.

$$\begin{cases} Nu = 0.023\, Re^{0.8} Pr^{0.4}, & Re > 10^4 \\ Nu = 4.36, & Re < 2300 \\ Nu = \dfrac{\left(\frac{f}{8}\right) \times Re \times Pr}{1.07 + 12.7\left(\frac{f}{8}\right)^{0.5} \times \left(Pr^{0.67} - 1\right)}, & 2300 < Re < 10^4 \end{cases} \tag{32}$$

To calculate the grout thermal resistance, Paul's model [36] was used. Paul used the so-called shape factor correlations, which were created by the experimental data and simulation results.

$$R_{grout} = \frac{1}{k_{grout}\beta_0 \left(\frac{d_b}{d_o}\right)^{\beta_1}} \tag{33}$$

where, β_0 and β_1 are dimensionless equation fit coefficients. d_b and d_o are diameter of borehole and outer diameter of pipe, respectively. Values of β_0 and β_1 are variable depending on the position of the tube in the grout. In this study typical values of $\beta_0 = 20.100377$ and $\beta_1 = -0.94467$ are considered [37].

3.2.5. Coupling vertical GHXs with heat pumps

Now, the heat pump must be coupled to the vertical GHX. Heat pump performance is affected mainly by four parameters of entering water temperature to the heat pump source and a load side and entering mass flow rate to those sides. In the present study, three parameters are constant and entering water temperature to the heat pump source side varies only. It means that the system performance is just a function of fluid temperature into the ground loop and varies in each time step concerning this value. As a result, outlet fluid temperature from vertical GHX couples the governing equations of heat pump performance and ground heat exchanger.

$$q(t) = \frac{\dot{Q}_{HP}}{N_b \cdot H} \times \left(1 - \frac{1}{COP(T_{f,in})}\right) \tag{34}$$

where N_b is the total number of boreholes and $\dot{Q}_{HP}$ is the amount of energy which is delivered by the heat pump. The $\dot{Q}_{HP}$ and COP are a function of inlet fluid temperature to heat pump source side and is determined by curve fitting of manufacturer's data. The COP and $\dot{Q}_{HP}$ are given as follows:

$$COP\left(T_{f,in}\right) = 0.0661 \cdot T_{f,in} + 2.7826 \tag{35}$$

In this study, it is assumed that first n-1 heat pumps are operating at full capacity while the n^{th} heat pump is at partial capacity. To easily include the PLF (part load factor), we just have to multiply the COP of the last heat pump not operating at full capacity by the part load factor and use the average COP [38].

$$COP_{pl} = COP\left(T_{f,in}\right) \cdot \frac{(n-1) + PLF}{n} \tag{36}$$

$$\dot{Q}_{HP}\left(T_{f,in}\right) = n_{HP} \cdot CAP\left(T_{f,in}\right) = n_{HP} \cdot \left(1620.9 \cdot T_{f,in} + 59746\right) \tag{37}$$

where CAP is the capacity of heat pumps. The strategy in this study is to scale up heat pump (from a reference model) in order to meet the heat load, then after the number of heat pump units are determined. For a given borehole configuration in simulation step, first the antifreeze solution temperature is guessed, then by using an FFT command in MATLAB the new inlet fluid temperature to the heat pump source side is estimated in the whole life of the proposed system. If the difference between the old and new temperature be greater than the specified value of 0.001 °C simulation process repeated with the new fluid temperature. The simulation is done until the temperature difference be lower than 0.001 °C.

3.3. Pumping power

Theoretical formulas could estimate calculation of consuming power by antifreeze solution pump, however, due to simplification of real condition they underestimate the power consumed by the pump. Thus, for establishing a condition near to reality, the pumping power is assumed to be 4% of heat load supplied by heat pumps (poor grade pump) [39].

After determining the consumed power by the fluid circulating pump, the whole system COP is also computed by:

$$COP_{sys} = \frac{\dot{Q}_{HP}}{\dot{W}_{pump} + \dot{W}_{HP}} \tag{38}$$

where $\dot{W}_{pump}$ and $\dot{W}_{HP}$ are the pump and GCHP power consumption respectiely.

4. Economic considerations

For investigation of the economic viability of the proposed system, the NPV, IRR (internal rate of return) and discounted payback period are used. They are used to decide whether to accept or reject investment projects.

In the simulation of the proposed system a number of design parameters such as the configuration of the boreholes, the number, the depth and the diameter of boreholes, the distance between the boreholes and the operating fluid mass flow rate flowing into each borehole could be addressed. The borehole configuration selected to be L-shaped, because its thermal performance relative to other configurations, i.e U-shaped, Squared shaped, is high [40]. The depth and number of the boreholes are determined via NPV analysis. In order to choose the borehole depth, the depth range is varied from 100 m to 150 m. About the distance of boreholes, it is recommended to select the value of the BH factor from 0.05 to 0.2, where the factor BH is defined as the ratio of distances between the boreholes to the depth of each borehole [41]. The value of BH adopted for this work is 0.1. Finally, by considering typical head loss of 0.4 *kPa/m* in the ground loop [42], mass flow rate in each borehole is given.

Table 1 details equipment costs used for economic analysis. The heat pump model used in the present study is WWG240 made in a commercial company of Iran. Purchase cost of this model is 17000 USD [43].

Inquiry of local deep drilling boreholes companies revealed that the cost of drilling varies in the range of 10–25 US$/m. Most companies claim that the deep boreholes up to 150 m depth can be delved for the price of 15 USD/m [44]. by considering the cost of preparing grout with thermal conductivity of 2 W/(m K) [45] and the cost of pipe and piping [17], the total cost of vertical GHX is estimated to be 20 USD/m. The electricity and NG cost are 0.1 *USD/kWh* and 0.07 *USD/m*^{3}.

5. Case study

To prove the suitability of the proposed system, thermal and economic performance study of the system is investigated under the condition of Kuhdasht CGS. The Kuhdasht is a county in Lorestan province (Iran). Mainly because of financial support from the Lorestan Gas Company, the city was selected as a case study.

The major information required for implementing the calculations and simulations necessary in this work are the mass flow rate, NG inlet temperature and pressure in Kuhdasht NG pressure drop station over a whole year. The database used for this work have been measured and recorded since 21 March 2013 to 20 March 2014, one year.

Fig. 3 shows daily mean mass flow rate in Kuhdasht. As can be seen, the gas flow rate increases through the CGS in the cold seasons of a year. It is mainly because of high heating demand provided by NG for buildings in Iran. Maximum gas flow rate recorded for the station is in the January with an amount of 4.4 kg/s. The minimum value is also 0.24 kg/s recorded at the June. Fig. 4 shows the main variable which causes the variation of inlet temperature to the turbo-expander. High inlet pressure rises the inlet temperature to turbo-expander and correspondingly the consumed energy in the NGEP. The maximum inlet pressure of turbo-expander is 6.7 MPa. Fig. 5 illustrates NG inlet temperature to the CGS. As expected, the least entrance temperatures belong to January (5 °C) and the highest temperature has been recorded in July (27.8 °C). In the winter, two negative factors lead to rising in energy consumption, high mass flow rate and low inlet temperature.

Table 1
Equipment costs.

Equipment	Cost (USD)
Turbo-expander [47]	$C = 1.3 \times 32100 \times \left(\frac{p_{elec}}{15}\right)^{0.6}$ $M = 0.02 \times C$
Heat Pump	17000
Fluid circulating pump [17]	$C = 271.64 \times \dot{m}_w + 1094.7$ ($)
Shell and tube heat exchanger [17]	$C = 549.56 \times A^{0.6691}$
Drilling, backfilling, pipe and piping	20 USD/m

For the Kuhdasht station based on thermodynamic relations and regarding NG composition (see Table 2) the hydrate formation temperature at the station exit pressure of 1.7 MPa is 5.7 °C. Therefore, by taking into account the confidence factor of 1.75, the temperature downstream of the turbo-expander is supposed to fix in 10 °C.

Lorestan Gas Company provided the other information related to the Kuhdasht CGS. Table 3 details the properties of the heater that employed in the Kuhdasht CGS. Table 4 also summarizes simulation parameters of the vertical GCHP.

6. Results and discussion

In this section, the simulation results of implementing the proposed system in Kuhdasht NG pressure drop station are presented.

6.1. Selecting a high benefit system

In heating mode of the heat pump, the low-temperature difference between the heat source and heating space leads to decrease in heat pump electricity demand. It in turn causes to increase the COP of the unit. Lowering the temperature difference in vertical GCHP entails that depth of boreholes together with the distance between adjacent boreholes rise. In his case study, as heat pump must supply a given heat load on the load side, the both factors cause to decrease in the number of purchased heat pump units. Yet, the high initial cost of drilling, piping, grout, fluid circulating pump and operational cost of the fluid circulating pump should also be considered. The mentioned issues have significant impacts on the profitability of the proposed system. On the other hand, a system with low borehole length not only results in running the heat pump with low-temperature fluid in source side but also increases the electricity demand of heat pump. Consequently, it lowers power delivered to the electricity grid and enhance the number of the required heat pump units. For this aim, the proposed system was simulated with a different number of boreholes and depth range of 100–150 m. The distances between adjacent boreholes are also allowed to vary in 0.1H to lower thermal interacting between boreholes in long time operation of GCHP. During the simulation process of the HPC-NGEP for finding the suitable number of the heat pump, borehole length and etc. Some VGHX systems which are not able to deliver fluid to heat pump in temperatures upper than −7 °C (the minimum temperature allowed by the heat pump manufacturer) in the lifetime of the system automatically are deleted in the simulation process.

Fig. 6 shows the NPV of the system against the total borehole length. As can be seen, the NPV fluctuates with increasing in the borehole length and not follow certain patterns. In considered range of borehole length, highest NPV obtained in total borehole length of 5700 m which corresponds to 38 boreholes in 150 m depth and 15 m distance between adjacent boreholes. Boreholes configuration is L-shaped, Fig. 7, with *Nx* and *Ny* equal to 20 and 18 respectively. The NPV obtained by this system is 644,000 $.

6.2. Performance of selected system

6.2.1. Heat extraction rate from the ground

Fig. 8 represent annually heat extraction rate from the ground. As expected, using ground just as a heat source caused to decrease continuously in absorbed heat from the ground. It is due to

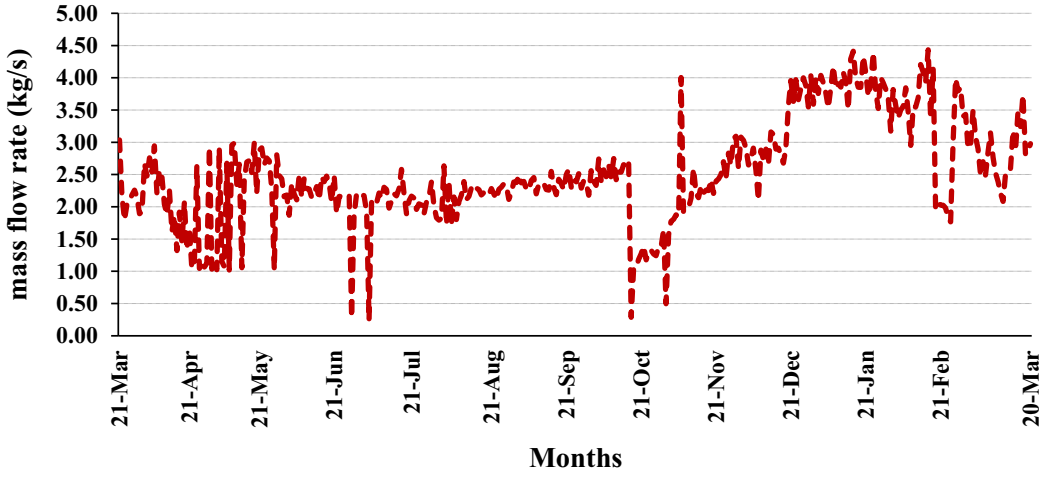

Fig. 3. Measured mass flow rate of NG passing through the Kuhdasht CGS.

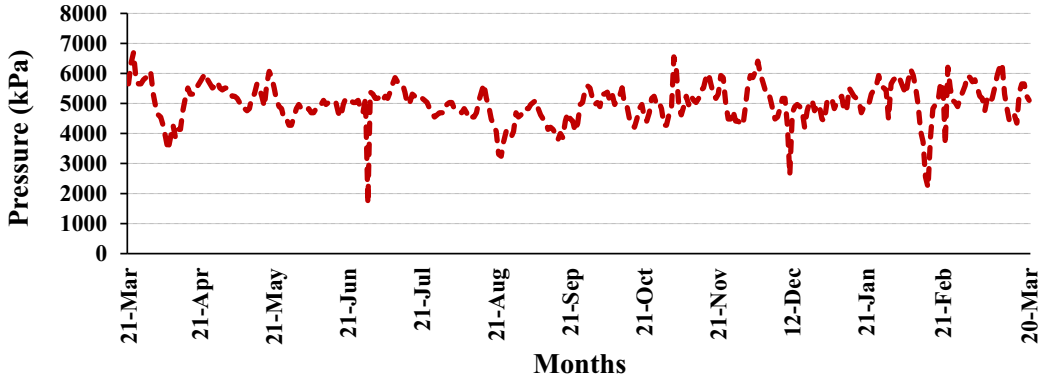

Fig. 4. Measured inlet pressure of NG to the Kuhdasht CGS.

decrease in the temperature difference between soil and pipe. The maximum and minimum heat extraction rates occur in the first and final year operation of the vertical GCHP respectively. Totally, absorbed heat in the first year is 1.25 GWh (25 W/m) while in the final year is 1.18 GWh (23.6 W/m). It corresponds to 5.6 percent decreasing in absorbing heat from the ground over the 25 years. It is worth noticing that low reduction of absorbed heat is because of the L-shaped arrangement of boreholes. It inherently has a high performance and long distance between adjacent boreholes (each borehole in 15 × 15 m grid). Vertical boreholes each in 4.5 × 4.5 m

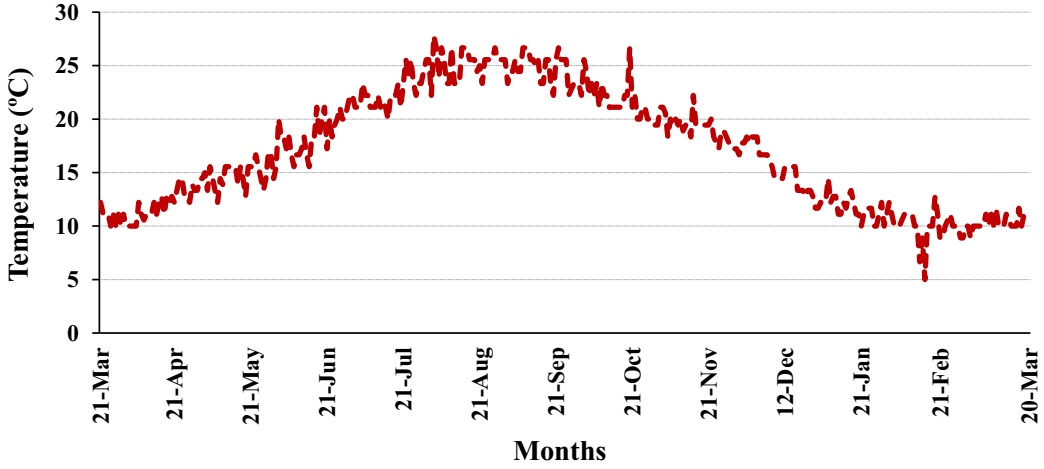

Fig. 5. Measured inlet temperature of NG to the Kuhdasht CGS.

Table 2
Chemical composition of Kuhdasht NG.

Composition	CH_4	C_2H_6	C_3H_8	n-C_4H_{10}	i-C_4H_{10}	n-C_5H_{12}	i-C_5H_{12}	C_6H_{14}	N_2	CO_2
Mole fraction (%)	87.7	4.7	1.74	0.42	0.37	0.1	0.13	0.08	4.7	0.05

Table 3
Properties of the Kuhdasht line heater.

Natural Gas Inlet Pressure	7 MPa
Natural Gas Outlet Pressure	1.7 MPa
Surface Area of Fire Tube Heater	88.1 m^2
Water Capacity	38 m^3
Diameter of Coil	0.1 m
Length of Coil	280 m
Heater Maximum Working Temperature	95 °C
Heater Maximum Heating Duty	1750 kW

Table 4
Parameters used in the simulation of the vertical GCHP.

d_i [cm]	2.04
d_o [cm]	2.5
k_{pipe} [$W/m\ K$]	0.42
d_b [cm]	15
k_{grout} [$W/m.K$]	2
H [m]	100-150
B [m]	0.1 × H
D [m]	3
T_g [°C]	20.5
k_g [W/$m.K$]	2.5
α [m^2/Day]	0.0876

grid have been recommended to prevent thermal interaction between boreholes [46]. Due to land availability in the CGS site long distance between boreholes is possible.

6.2.2. Annually delivered power to the electricity grid

The vertical GCHP annually provide 1.74 GWh energy to NG passing through the shell and tube heat exchanger. As understood, the heat extraction rate from the ground reduces annually. To compensate this heat extraction from the ground, the heat pump will consume more electricity yearly. Over 25 years, the heat pump electricity demand will be increased by 14.7 percent and reached from 0.49 GWh to 0.56 GWh, shown in Fig. 9.

Increasing GCHP power consumption will cause to the smaller amount of net power delivered to the electricity grid, shown in Fig. 10. Thus, the profitability of the proposed system will decline by decreasing the net power delivered to the grid. Antifreeze solution which is being circulated by the pump is another power consuming unit. Totally, both units affect the profitability of the project and decrease the net power over the system lifetime. The decreased net power amount over the life of the system is 71.66 MWh.

6.2.3. Mean annually COP of the whole system and GCHP

Heat pump COP is affected by entering fluid temperature to source side (evaporator). By increasing the evaporator inlet temperature, the performance of the vertical GCHP go up. It means that the heat pump needs smaller amounts of electricity for the compressor. In the present study, continuously heat extraction will degrade the energy level of the ground. As can be seen in Fig. 11 the heat transfer fluid temperature and temperature around the boreholes will decrease over the system lifetime. The graph shows the mean outgoing fluid temperature from the ground loop against the GCHP and the whole system COP. It should be noted that fluid circulator pump power is also taken into account in calculating the system COP. It reveals that the GCHP mean COP is always greater than 3 and determined to be in the range of 3.18–3.65. For the whole system, mean COP is in the range of 2.83–3.20. Mean outgoing fluid temperature from VGHX during the first year and final year are 13.18 °C and 6 °C respectively. A minimum antifreeze solution temperature of −0.3 °C was observed in 25 years simulation.

6.2.4. Energy performance analysis

Fig. 12 shows a comparison between the line heater heating duty of conventional NGEP and HPC-NGEP during one year. The high heating duty of conventional NGEP in cold seasons is obvious. It is mainly because of higher NG mass flow rate and low-temperature gas at the entrance of the heater. The heating duty of the heater in January reaches to the monthly peak value of

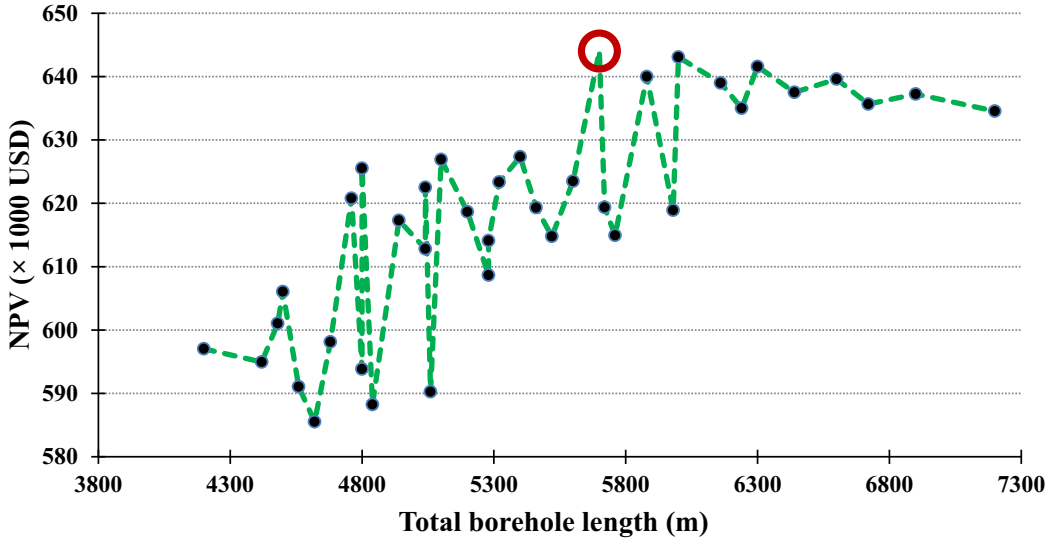

Fig. 6. Selecting a system with high NPV.

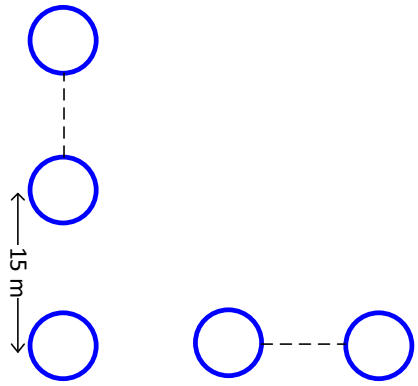

Fig. 7. Selected L-shaped configuration.

1.71 TJ, while by employing the vertical GCHP the value reduces to 0.77 TJ.

It is worth noticing that annual heater heating duty of HPC-NGEP will be unchanged over the 25 years running the system. The annual heating duty of HPC-NGEP is 5.17 TJ. To keep heater heating duty of HPC-NGEP unchanged, the number of running heat pumps go up year by year. In other word, for supplying yearly constant heat load by GCHP, a number of heat pumps are going up to compensate for the reduction of absorbed heat from the ground.

Fig. 13 illustrates the total monthly energy is providing a contribution of vertical GCHP and the line heater in the proposed system. As can be seen, the geothermal system could reduce energy consumption of the NGEP up to 52.50% (in July). Minimum energy reduction is also 39% and occurs in February. Totally, yearly average energy consumption reduction of 45.80% is obtained by employing the geothermal system.

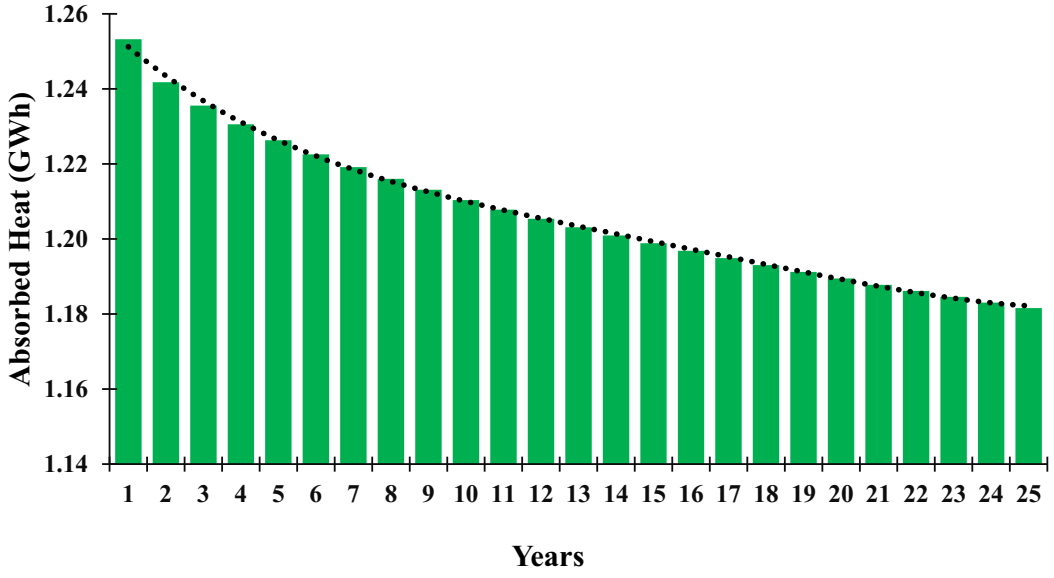

Fig. 8. Heat Extraction Rate from the ground.

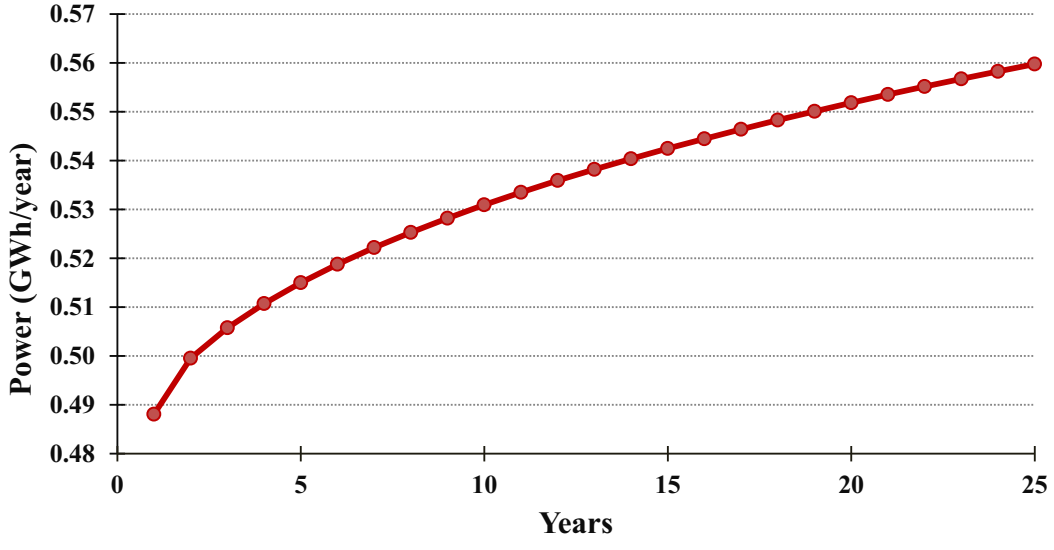

Fig. 9. Vertical GCHP electricity consumption.

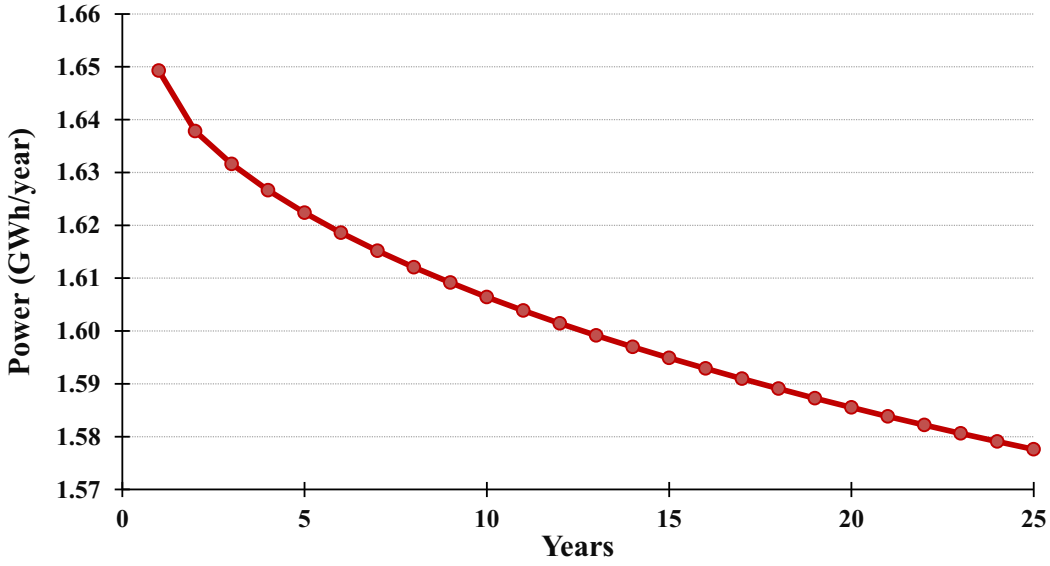

Fig. 10. Electricity power delivered to the electricity grid.

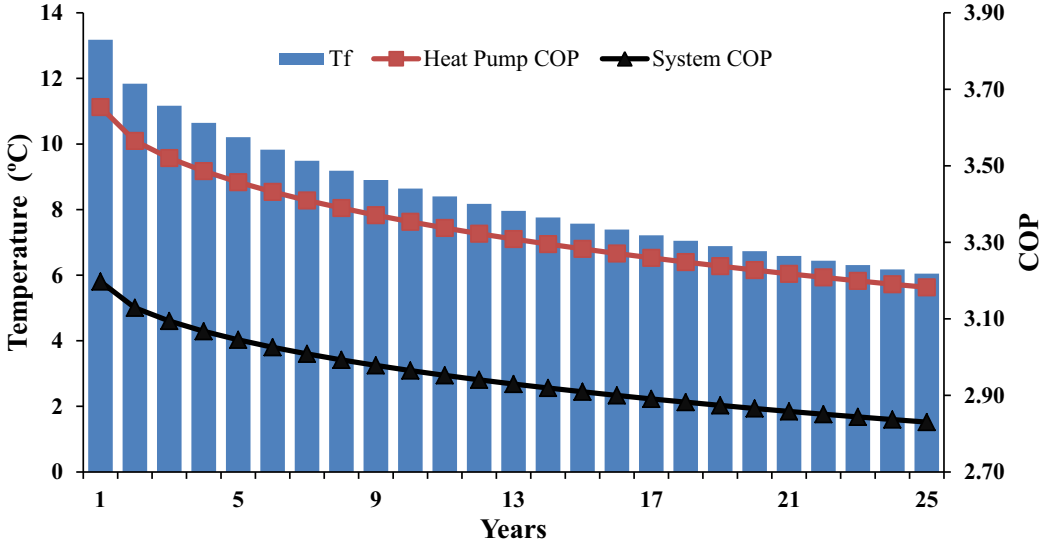

Fig. 11. COP of heat pump and system versus mean fluid temperature of ground loop.

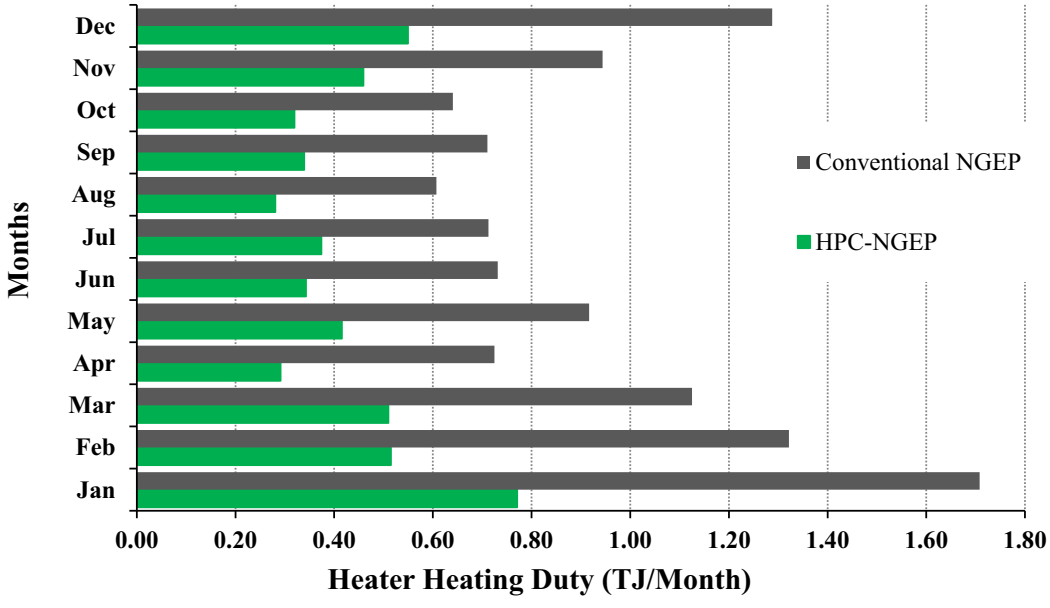

Fig. 12. Line heater heating duty of NGEP and HPC-NGEP.

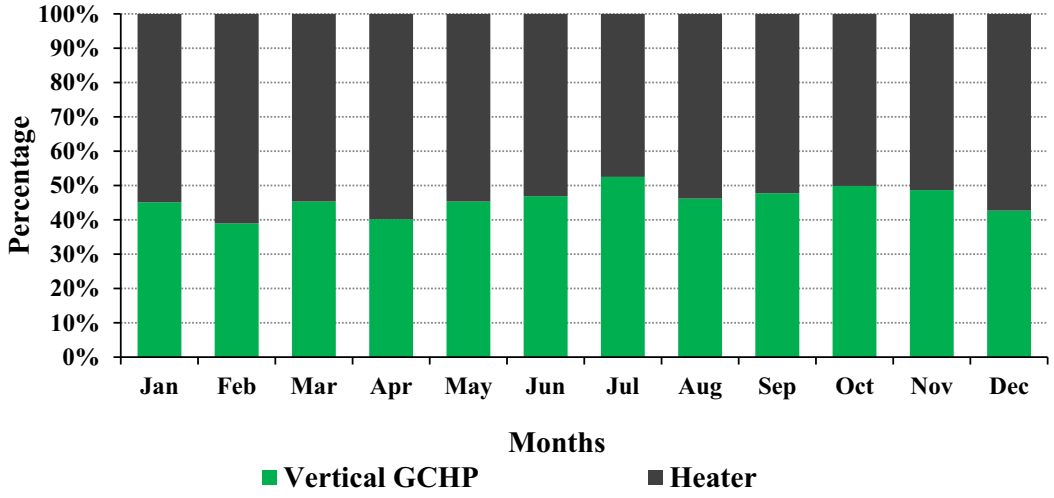

Fig. 13. Total monthly energy providing contribution of vertical GCHP and line heater.

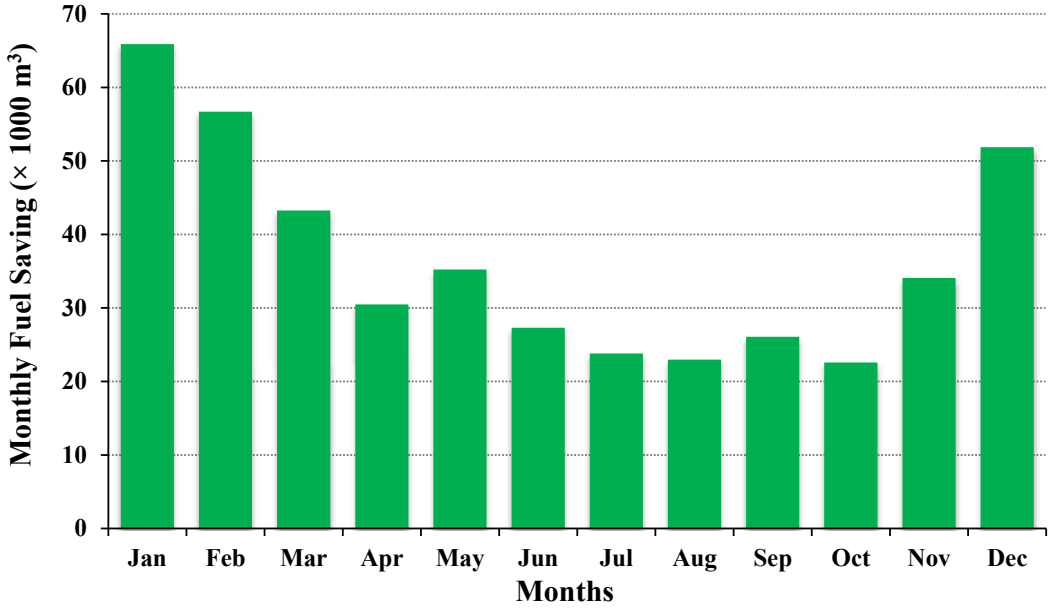

Fig. 14. Total Monthly fuel consumption saving of the HPC-NGEP.

The heating duty difference (see Fig. 12) is directly related to fuel consumption saving. Fig. 14 shows the Monthly fuel consumption saving of HPC-NGEP. Monthly fuel consumption saving is in the range of (22578–65887) nm^3.

Preheating of the NG stream in the NGEP is just done with line heater. It burns 803595.46 nm^3 of NG annually where 102702187 nm^3 of gas is passed through the expander over one year. It represents that approximately 0.78% of the total gas flow through the CGS must be burned to produce sufficient heat. The obtained value is three times higher than the value reported by of Howard et al. [18]. They showed the mentioned amount was about 0.26% for single turbo-expander and boiler system. The main reasons for this significant differences are: 1) thermal efficiency of boiler used by them is two times higher than line heater efficiency

Table 5
Thermal efficiency of the NGEP and HPC-NGEP.

System	Jan	Feb	Mar	Apr	May	Jun	Jul	Aug	Sep	Oct	Nov	Dec	Mean
HPC-NGEP (1st year)	40.21	43.04	40.14	46.19	44.63	48	47.41	59.19	55.87	48.78	46	46.16	47.14
HPC-NGEP (25th year)	38.17	40.47	37.98	43.27	42.49	46.1	55.62	54.24	47.31	44.44	44.44	44.03	44.88
NGEP ($\eta_h = 40\%$)	24.76	24.07	24.39	24.94	26.15	28.29	29.91	33.02	32.22	29.65	27.95	26.29	27.64
NGEP ($\eta_h = 80\%$)	49.52	48.14	48.78	49.88	52.3	56.58	59.82	66.04	64.44	59.30	55.9	52.58	55.27

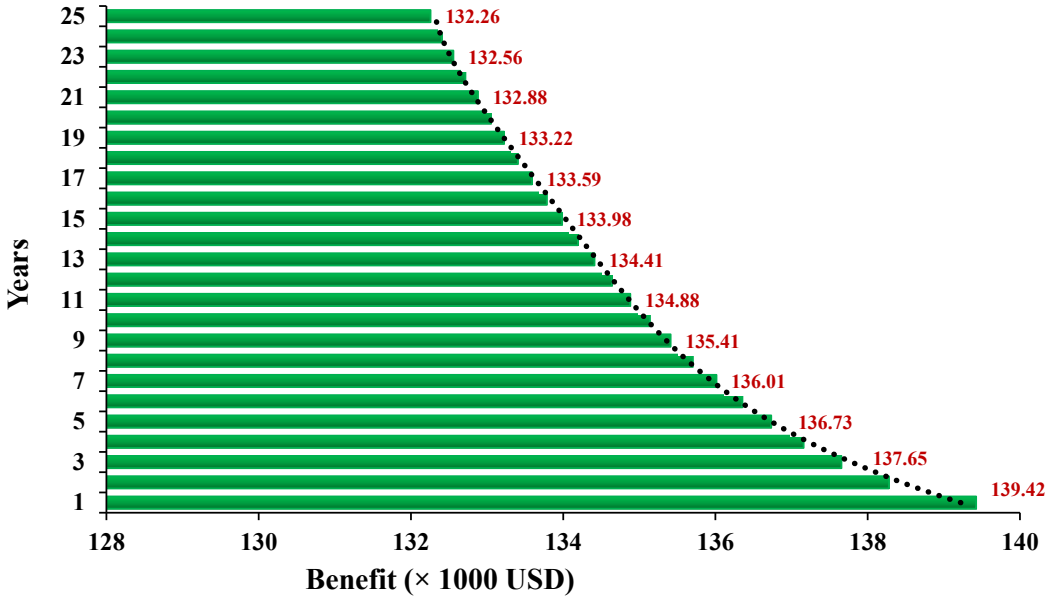

Fig. 15. The total annual achievable benefit of employing the HPC-NGEP.

and 2) the turbo-expander downstream temperature assumed by them is three times lower than the present study, which reduces preheating energy.

The proposed system shows better results in terms of reduction in fuel consumption. It annually burns just 363,334.35 nm^3 of NG, fuel saving by the proposed system is noticeable. The amount of fuel consumed by the system is about 0.35% of the total NG flow passed through the CGS over the year. The value of 0.26% reported by Howard et al. [18] is also higher than the obtained value (0.35%) in this study.

Table 5 details the thermal efficiency of the NGEP and HPC-NGEP. Thermal efficiency is defined as the ratio of power delivered to the electricity grid to the energy required by the system. Therefore, it is defined such as $P_{ele}/(\dot{m}_{fuel}\cdot LHV)$ and $P_{net}/(\dot{m}_{fuel}\cdot LHV)$ for NGEP and HPC-NGEP respectively.

Illustrating the variation of the thermal efficiencies for the HPC-NGEP over the lifetime of the system, it is presented at first and 25th year. According to Table 5, the yearly average thermal efficiency of HPC-NGEP is reduced from 47.14% in the first year to 44.88% in the 25th year. In the other words, the thermal efficiency in 25 years operation of the system decreases just 2.26%. By comparing the thermal efficiency of the conventional NGEP and proposed system, it is founded, employing the vertical GCHP could increase thermal efficiency (1.6–1.7) times (yearly average).

The low thermal efficiency of the systems is mainly because of the low thermal efficiency of the line heater. By doubling the line

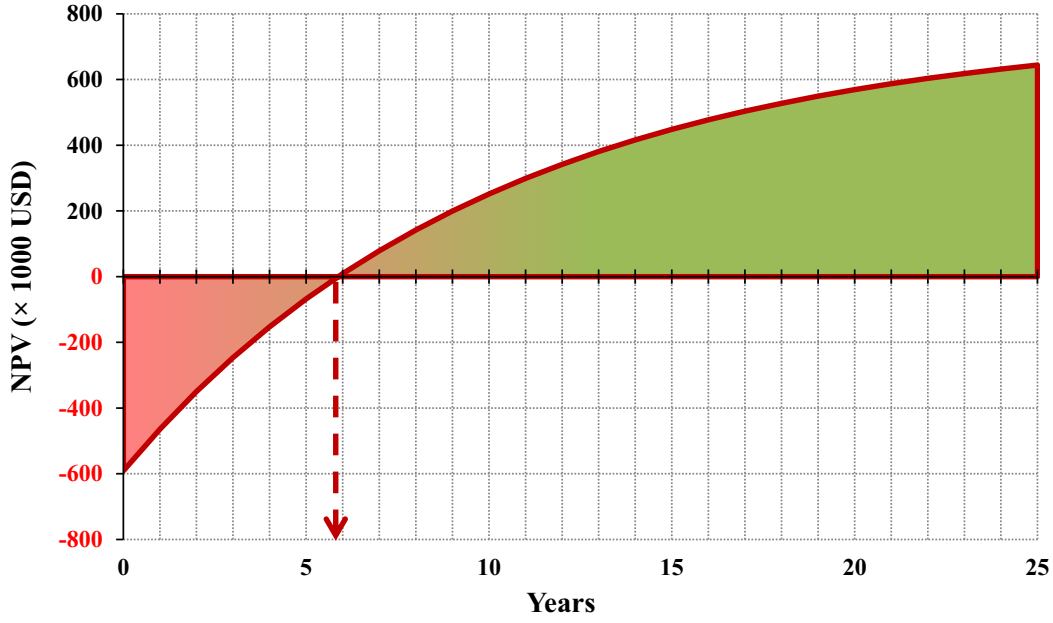

Fig. 16. The NPV analysis of the proposed system.

heater thermal efficiency from 40% to 80% (last row of Table 5) thermal efficiency of the conventional NGEP is also becomes two times. In this case, the yearly average thermal efficiency is increased from 27.64 to 55.27%. The obtained value is higher than the thermal efficiency of the HPC-NGEP. Thus, employing vertical GCHP with high thermal efficiency heater could give better results.

6.2.5. Economic aspects of proposed system

Fig. 15 shows total achievable yearly benefit from employing the HPC-NGEP over the lifetime of the system. The descending behavior of achieving benefit is because of the reduction in power delivered to the electricity grid. Although, the annual benefit of the system decreases over time, even after 25 years, the system still works impressively.

Fig. 16 illustrates the discounted payback period of the system on a basis of the NPV method employing the achievable yearly profits. In this assessment, the inflation rate has been considered 10%. Capital cost and NPV of the system are 590,940 $ and 644,000 $ respectively. The discounted payback period is 5.87 years, and the internal rate of return is also 23%. As the least period for the efficient performance of such systems has been defined over 25 years, this value, by itself, can be a strong evidence of the suitability of the proposed system.

7. Conclusion

NG is delivered to the end consumers through a long pipeline network. It is transferred in pressures as high as 5–7 MPa. However, end consumers need to use the low-pressure level NG, Therefore, the pressure decreases in several stages. The main pressure drop stage accomplished in the conventional pressure drop stations by throttling valve. Through the throttling process, a large amount of pressure exergy is wasted. The modern pressure drop stations known as NGEPs use the pressure exergy for producing electrical power, however; high preheating energy demand compared to the conventional type is a major issue with them.

A new system was proposed to lower the energy consumption of the NGEP. The system takes the advantage of geothermal energy by using a vertical GCHP. The turbo-expander provides the GCHP and electricity demand and pumping power. Economic results showed a system with total borehole length of 5700 m in the L-shaped configuration. It is found that eight heat pumps have a higher NPV between other systems with different borehole lengths. The whole system and GCHP COP were determined in the range of 2.83–3.20 and 3.18–3.65 respectively. Average yearly fuel consumption reduction was predicted about 45.80%. Obtained economic parameters also proved that the presented system could be suitable for the NGEP. The IRR and discounted payback period were 23% and 5.87 years respectively.

Nomenclature

q	heat flux (W/m)
H	active borehole length (m)
R	thermal resistance
f	friction coefficient
d	diameter (m)
D	inactive borehole length (m)
B	borehole distance (m)
m_w	the line heater water mass (kg)
c_f	antifreeze solution specific heat
T_f	antifreeze average temperature at the ground heat exchanger (°C)
$T_{f,in}$	antifreeze solution temperature at the ground heat exchanger outlet (°C)
$T_{f,out}$	antifreeze solution temperature at the ground heat exchanger inlet (°C)
N_b	number of boreholes
C_w	the line heater water thermal capacity
$C_{p,NG}$	natural gas thermal capacity
$\dot{m}_f$	the mass flow rate of antifreeze solution (kg/s)
$\dot{m}_{NG}$	the mass flow rate of natural gas passing through the station (kg/s)
$\dot{Q}_{NG}$	heat absorbed by the natural gas when passes through line heater (kW)
$\dot{Q}_{HP}$	heat delivered to system with heat pump (kW)

Greek letters

η_{ex}	isentropic efficiency of turbo-expander
γ	specific heat ratio of natural gas
η_{gear}	efficiency of gear
η_{gen}	efficiency of generator
η_h	thermal efficiency of line heater
α	soil thermal diffusivity
F	fast Fourier Transform

Subscripts

NG	natural Gas
ex	turbo-expander
elec	electrical
b	borehole
Conv	convection
Cond	conduction
in	inlet
i	inner
o	outer
g	ground
bw	borehole wall

References

[1] Zarrella A, Capozza A, De Carli M. Analysis of short helical and double U-tube borehole heat exchangers: a simulation-based comparison. Appl Energy 2013;112:358–70.
[2] Fujii H, Nishi K, Komaniwa Y, Chou N. Numerical modeling of slinky-coil horizontal ground heat exchangers. Geothermics 2012;41:55–62.
[3] Michopoulos A, Bozis D, Kikidis P, Papakostas K, Kyriakis NA. Three-years operation experience of a ground source heat pump system in Northern Greece. Energy Build 2007;39:328–34.
[4] Ozyurt O, Ekinci DA. Experimental study of vertical ground-source heat pump performance evaluation for cold climate in Turkey. Appl Energy 2011;88:1257–65.
[5] Zhai XQ, Yang Y. Experience on the application of a ground source heat pump system in an archives building. Energy Build 2011;43:3263–70.
[6] BP Statistical Review of World Energy. 2014.
[7] Farzaneh-Gord M, Hashemi S, Sadi M. Energy destruction in Iran's natural gas pipe line network. Energy Explor Exploit 2007;25:393–406.
[8] Farzaneh-Gord M, Rahbari HR, Bajelan M, Pilehvari L. Investigation of hydrate formation in natural gas flow through underground transmission pipeline. J Nat Gas Sci Eng 2013;15:27–37.
[9] Farzaneh-Gord M, Arabkoohsar A, Deymi Dasht-bayaz M, Farzaneh-Kord V. Feasibility of accompanying uncontrolled linear heater with solar system in natural gas pressure drop stations. Energy 2012;41:420–8.
[10] Querol E, Gonzalez-Regueral B, García-Torrent J, Ramos A. Available power generation cycles to be coupled with the liquid natural gas (LNG) vaporization process in a Spanish LNG terminal. Appl Energy 2011;88:2382–90.
[11] Kargaran M, Arabkoohsar A, Hagighat-Hosini SJ, Farzaneh-Kord V, Farzaneh-Gord M. The second law analysis of natural gas behavior within a vortex tube. Therm Sci 2013;17:1079–92.
[12] Farzaneh-Gord M, Arabkoohsar A, Deymi Dasht-bayaz M, Machado L, Koury RNN. Energy and exergy analysis of natural gas pressure reduction points equipped with solar heat and controllable heaters. Renew Energy 2014;72:258–70.
[13] Farzaneh-Gord M, Ghezelbash R, Arabkoohsar A, Pilevari L, Machado L, Koury RNN. Employing geothermal heat exchanger in natural gas pressure drop station in order to decrease fuel consumption. Energy 2015;83:164–76.

[14] Požívil J. Use of expansion turbines in natural gas pressure reduction stations. Acta Montan Slovaca 2004;3:258–60.
[15] Farzaneh-Gord M, Maghrebi MJ. Exergy of natural gas flow in Iran's natural gas fields. Int J Exergy 2009;6:131–42.
[16] Farzaneh-Gord M, Deymi-Dashtebayaz M. Effect of various inlet air cooling methods on gas turbine performance. Energy 2011;36:1196–205.
[17] Sanaye S, Mohammadi Nasab A. Modeling and optimizing a CHP system for natural gas pressure reduction plant. Energy 2012;40:358–69.
[18] Howard C, Oosthuizen P, Peppley B. An investigation of the performance of a hybrid turboexpander-fuel cell system for power recovery at natural gas pressure reduction stations. Appl Therm Eng 2011;31:2165–70.
[19] Kostowski WJ, Usón S. Comparative evaluation of a natural gas expansion plant integrated with an IC engine and an organic Rankine cycle. Energy Convers Manag 2013;75:509–16.
[20] Farzaneh Gord M, Jannatabadi M. Simulation of single acting natural gas reciprocating expansion engine based on ideal gas model. J Nat Gas Sci Eng 2014;21:669–79.
[21] Neseli MA, Ozgener O, Ozgener L. Energy and exergy analysis of electricity generation from natural gas pressure reducing stations. Energy Convers Manag 2015;93:109–20.
[22] Arabkoohsar A, Farzaneh-Gord M, Deymi-Dashtebayaz M, Machado L, Koury R. A new design for natural gas pressure reduction points by employing a turbo expander and a solar heating set. Renew Energy 2015;81:239–50.
[23] Marcotte D, Pasquier P. The effect of borehole inclination on fluid and ground temperature for GLHE systems. Geothermics 2009;38:392–8.
[24] Farzaneh-Gord M, Rahbari H. Developing novel correlations for calculating natural gas thermodynamic properties. Chem Process Eng 2011;32:435–52.
[25] Incropera FP. Fundamentals of heat and mass transfer. John Wiley & Sons; 2011.
[26] Bernier MA. Ground-coupled heat pump system simulation. ASHRAE Trans 2001;107:605–16.
[27] Li M, Li P, Chan V, Lai AC. Full-scale temperature response function (G-function) for heat transfer by borehole ground heat exchangers (GHEs) from sub-hour to decades. Appl Energy 2014;136:197–205.
[28] Ingersoll LR, Zabel OJ, Ingersoll AC. Heat conduction with engineering, geological, and other applications. 1954.
[29] Zeng H, Diao N, Fang Z. A finite line-source model for boreholes in geothermal heat exchangers. Heat Transfer Asian Res 2002;31:558–67.
[30] Cimmino M, Bernier M. Preprocessor for the generation of g-functions used in the simulation of geothermal systems. In: 13th Conference of the International Building Performance Simulation Association (IBPSA); 2013. p. 2675–82.
[31] Eskilson P. Thermal analysis of heat extraction boreholes. Lund University; 1987.
[32] Lamarche L, Beauchamp B. A new contribution to the finite line-source model for geothermal boreholes. Energy Build 2007;39:188–98.
[33] Claesson J, Javed S. An analytical method to calculate borehole fluid temperatures for time-scales from minutes to decades. ASHRAE Trans 2011;117:279–88.
[34] Pasquier P, Marcotte D. Efficient computation of heat flux signals to ensure the reproduction of prescribed temperatures at several interacting heat sources. Appl Therm Eng 2013;59:515–26.
[35] Marcotte D, Pasquier P. Fast fluid and ground temperature computation for geothermal ground-loop heat exchanger systems. Geothermics 2008;37:651–65.
[36] Paul ND. The effect of grout thermal conductivity on vertical geothermal heat exchanger design and performance. South Dakota State University; 1996.
[37] Yavuzturk C, Spitler J, Rees S. A transient two-dimensional finite volume model for the simulation of vertical U-tube ground heat exchangers. ASHRAE Trans 1999;105:465–74.
[38] Bettanini E, Gastaldello A, Schibuola L. Simplified models to simulate part load performances of air conditioning equipments. In: 8th International IBPSA conference, Eindhoven, Netherland; 2003.
[39] Kavanaugh SP, Rafferty KD. Ground-source heat pumps: design of geothermal systems for commercial and institutional buildings. American Society of Heating, Refrigerating and Air-Conditioning Engineers; 1997.
[40] Casetta D. Implementation and validation of a ground source heat pump model in MATLAB. 2012.
[41] Gultekin A, Aydın M, Sisman A. Determination of optimal distance between boreholes.
[42] Robert F, Gosselin L. New methodology to design ground coupled heat pump systems based on total cost minimization. Appl Therm Eng 2014;62:481–91.
[43] Accessed 2014; http://www.bernoulli.ir/.
[44] http://shaft-dig.blogfa.com/.
[45] Allan M. Thermally conductive cementitious grout for geothermal heat pump systems. Google Patents; 2001.
[46] Michopoulos A, Kyriakis N. Predicting the fluid temperature at the exit of the vertical ground heat exchangers. Appl Energy 2009;86:2065–70.
[47] Kostowski WJ, Usón S, Stanek W, Bargiel P. Thermoecological cost of electricity production in the natural gas pressure reduction process. Energy.